Experimental investigation of volatiles-bed contact in a 2-4MWth bubbling bed reactor of a dual fluidized bed gasifier

Teresa Berdugo Vilches, Henrik Thunman*

Department of Energy and Environment, Division of Energy Technology, Chalmers University of Technology, SE-41296 Gothenburg, Sweden

KEYWORDS

Fluidized bed, biomass, volatiles-bed contact, oxygen carrier

ABSTRACT

The use of catalytic bed materials in fluidized bed gasifiers represents a promising primary measure to decrease the tar content of biomass-derived raw gas. For effective application of such in-bed catalysts, extensive contact must be established between the volatile matter released from the fuel particles and the bed material. However, the extent of the contact and, consequently, the potential of in-bed tar removal techniques, are not well understood. In this work, the fraction of volatile matter that interacts with the bed in a large (i.e., throughput of 300–400 kg/h biomass) bubbling bed gasifier is quantified experimentally, and the effect of fluidization velocity is investigated. The results show that a higher fluidization velocity enhances gas-solid contact, with 48%–69% of the volatile matter coming in contact with the bed within the range of 6–10-times the minimum fluidization (u_{mf}).

1. INTRODUCTION

Fluidized bed reactors have been extensively investigated and applied in industry owing to their versatility and their suitability for large-scale operation [1]. In the energy sector, this type of reactor has been in common use since the 1980s for the combustion of non-homogeneous fuels [2]. In addition, some fluidized bed systems have been constructed for the gasification of solid fuels on commercial and demonstration scales [3], and more recently, for chemical looping combustion (CLC) [4]. Among their advantages, fluidized beds offer the possibility to use additives or active materials that improve fuel conversion and/or decrease the levels of unwanted species, thereby reducing the need for extensive gas conditioning and simplifying the plant design. In the context of biomass gasification, the major undesirable species are condensable hydrocarbons, commonly referred to as 'tar'. These compounds cause fouling of the downstream equipment and restrict the final application of the product gas. Several active materials, including dolomite and olivine, have been investigated in fluidized beds for the prevention of build-up of tar compounds; and the results are presented in comprehensive reviews in the literature[5, 6].

The effective use of catalysts in large gasifiers depends not only on their physical and chemical properties, but also on the operational conditions and gasifier configuration. The latter ultimately affects the mixing of the bed inventory and the volatiles released from the solid fuel particles, which is a crucial parameter when gas-solid interactions are required. The geometry of the reactor, for instance, can influence the level of turbulence and promote back-mixing of the gas and solids. A gasifier design that is based on this principle, which divides the reactor into sections using a sequence of necks to enhance gas-solids contacts, has been proposed by Pfeifer and co-workers [7, 8]. The location of the fuel-feeding point has also been proven to have an impact on gas-solids contacts. Improved gas conversion through the use of in-bed, as compared to over-bed, fuel feeding has been reported by Wilk et al. [9] for steam

gasification of wood pellets in a 100-kW dual fluidized bed pilot plant. However, the relevance of this effect is most likely affected by the size of the reactor.

In terms of operational conditions, a higher fluidization velocity is known to intensify particle ejection into the freeboard [10], which makes turbulent and fast fluidization the preferable regimes when extensive gas-solid contact is desired. Bubbling beds are, however, a common design of fluidized bed gasifiers, such as in dual fluidized bed (DFB) systems, where the gasification reactor operates in the bubbling regime. Such reactor arrangement together with the highly volatile nature of biomass fuels has inherent limitations with respect to fuel mixing and, consequently to gas-solid contact. In particular, there is a tendency for devolatilizing fuel particles to concentrate at the vicinity of the bed surface. This phenomenon, which is known as segregation, is the result of differences in properties of the bed material compared to the fuel particles[11], and it is further enhanced by the formation of volatile bubbles around the devolatilizing fuel particle[12, 13]. The volatile bubbles (i.e. endogenous bubbles) induce a lifting force over the devolatilizing fuel and contribute to keep it floating [14]. When the rise of the fuel particles through the bed is rapid compared to devolatilization, the volatiles are released directly into the splashing zone and/or the freeboard regardless the location of the fuel feeding point. This causes maldistribution of the volatiles in the reactor. After devolatilization, the remaining char is likely to move downwards and mix with the bed [15].

The maldistribution of volatiles has been subject of numerous works related to combustion of high-volatile fuels, since it causes uneven temperature profiles throughout the reactor and undesired emissions. The release of volatiles at the top of the bed leads, for instance, to significant heat release in the splash and/or freeboard region, as predicted by a number of models developed in the context of fluidized bed combustion of high volatile fuels[16-19]. In fluidized bed gasifiers, the release of volatiles directly into the splash zone and/or the freeboard causes poor gas-solid contact and limit the effectiveness of the above mentioned

catalysts for tar removal when they are applied inside the gasifier. The poor gas-solid contact is expected to be even more pronounced in gasifiers that have over-bed fuel-feeding systems, since the fuel particles are most likely located in the upper region of the bed during the whole devolatilization time. Figure 1 illustrates a top-view of a bubbling bed gasifier with an over-bed fuel-feeding system that is operated at lower and higher fluidization velocities. At a low fluidization velocity, there is clear evidence of segregation and accumulation of the fuel particles, whereas at a higher fluidization velocity, there is visually better fuel mixing. The extent of mixing of the volatiles emitted from the fuel particles and the bed material in bubbling bed reactors is not straightforward, and the present work constitutes an attempt to throw light on this issue.

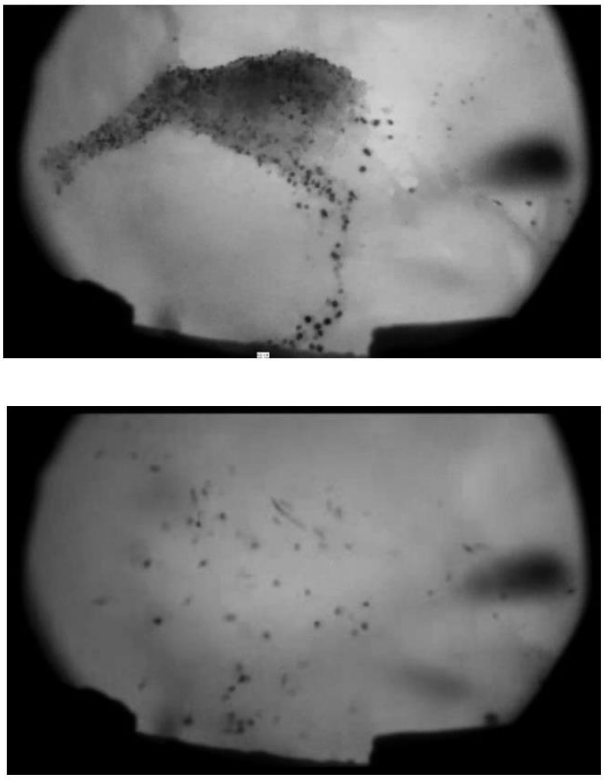

Figure 1. Top-view of the Chalmers gasifier fluidized with steam and fed with wood pellets (top panel: uo~0.15 m/s; bottom panel, uo~0.20 m/s). Fuel particles are evident as black dots and the bed material appears as the gray background.

In this investigation, gas-solid contacts are traced by taking advantage of the fast oxidation of volatiles by an oxygen carrier material widely used in CLC research. Oxygen carriers are typically metal oxides (MeO) that undergo redox cycles when alternately exposed to oxidizing and reducing atmospheres. During such cycles, the MeO undergoes a number of physical and/or chemical changes (commonly referred to as activation) that affect its reactivity. In a CLC unit, oxygen is transported by the bed material, which circulates between two interconnected fluidized bed reactors (i.e., the fuel and air reactors). Initially, the bed material is oxidized by reaction with oxygen in the air reactor (R1). Thereafter, the oxidized bed material is transported into the fuel reactor, where the solid fuel particles devolatilize (R2) and the remaining char is gasified (R3). Finally, the gas species are combusted by reaction with the oxygen carrier (R4 and R5), which is envisioned as a heterogeneous (gas-solid) reactions [20].

$$Me + \frac{1}{2}O_2 \rightarrow MeO \quad \text{(R1)}$$

$$Biomass \rightarrow Volatile\ matter + Char + H_2O \quad \text{(R2)}$$

$$Char + H_2O \rightarrow Gasification\ products + ash \quad \text{(R3)}$$

$$Gasification\ products + MeO \rightarrow CO_2 + H_2O + Me \quad \text{(R4)}$$

$$Volatile\ matter + MeO \rightarrow CO_2 + H_2O + Me \quad \text{(R5)}$$

Provided that the oxygen carrier is highly oxidized, every contact event between the combustible gases and bed particles results in an exchange of oxygen. The oxygen consumed by the gas is, consequently, proportional to the volatile-bed contacts.

The aim of the present work is to estimate the fraction of volatiles released from a large solid fuel particle that comes in contact with the bed material in a bubbling bed reactor. For this purpose, an experimental method is developed, and the major uncertainties are identified and

investigated. The main focus of this study is to explore the impact of fluidization velocity on volatiles-bed contacts within the bubbling regime, while providing results that are relevant to industrial-scale units with over-bed fuel-feeding systems.

2. METHODOLOGY

To estimate the fraction of volatiles that meets the bed material, an oxygen carrier was used in a dual fluidized bed (DFB) gasifier. Figure 2 depicts a simplified sketch of the process and the path of the oxygen carrier in it. The combustor operates as a circulating bed, whereas the gasifier operates a bubbling regime with moderate gas velocities (u_o). To ensure a bubbling regime u_o is kept above minimum fluidization velocity (u_{mf}) of the largest bed particle size and below the terminal velocity (u_t) of the smallest fraction of the bed particles in the reactor[1].

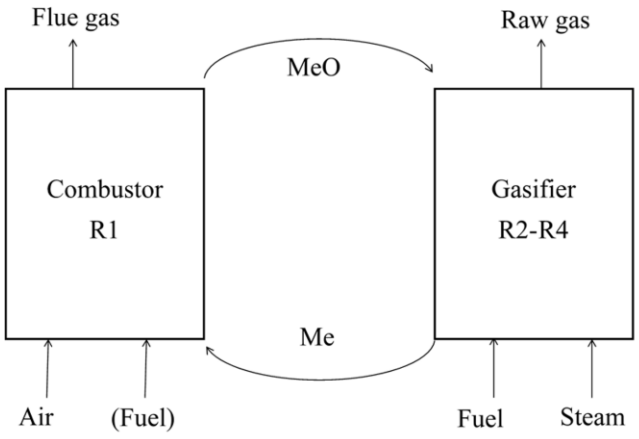

Figure 2. Schematic of a dual fluidized bed indirect gasifier that uses an oxygen carrier as the bed material

Ilmenite as an oxygen carrier. The selected bed material was ilmenite, which is a naturally occurring iron-titanium ore that has been investigated for its high oxygen-carrying capacity[21-23]. The oxygen-carrying capacity (R_o) of ilmenite depends on its activation, being typically 3.3%–2.1% (on a mass basis) for the activated material[22-24]. Activation of ilmenite is

characterized by an increase in porosity and the migration of iron to the surface of the particle[23].

For a given fuel flow ($\dot{m}_F$), R_o, and bed material flow ($\dot{m}_{ilm}$), the amount of oxygen carried by the solids into the gasifier can be expressed as a fraction of the stoichiometric oxygen required for full combustion of the fuel (Ω_{SF}) as follows:

$$\lambda = \frac{\dot{m}_{ilm} \cdot R_o}{\dot{m}_F \cdot \Omega_{SF}} \quad (1)$$

This parameter is hereinafter referred to as 'oxygen availability' and denoted by the symbol λ, owing to its resemblance to the air-to-fuel equivalence ratio in traditional combustion systems. Operation at well above the stoichiometric condition (λ>1) is required to ensure that incomplete combustion does not result from a lack of oxygen in the gasifier, and the bed material flow ($\dot{m}_{ilm}$) has to be adjusted for this purpose.

Ilmenite as a catalyst. Insufficient oxygen inevitably leads to higher levels of reduced iron in the bed inventory (e.g., Fe^0, Fe^{+2}), which have been reported to catalyze reforming, tar cracking, and Water-Gas-shift (WGS) reactions[25-28]. As a consequence, some of the combustible gases released in the gasifier may interact with the bed particles that have already lost their content of oxygen and participate in catalytic reactions, in which case the volatiles-bed contact cannot be traced by an exchange of oxygen. Therefore, it is important to verify that the gas composition at the exit of the reactor shows trends that are in line with dominant combustion reactions. Complete gas analysis including tar samples was taken to gain insights into the relevance of the catalytic and oxidation reactions mediated by the MeO.

Char conversion. The raw gas that exits the gasifier originates from both devolatilization and char gasification products. Quantification of char conversion, which is important with regard

to understanding the contribution of volatiles to the measured gas yield, can be performed using a carbon balance across the gasifier, as follows:

$$X_{char} = \frac{Y_{char} - (Y_{C,fuel} - Y_{C,raw\ gas}) \cdot \left(1 + \left[\frac{H}{C}\right]_{UC} + \left[\frac{O}{C}\right]_{UC}\right)}{Y_{char}} \qquad (2)$$

where Y_{char} denotes the char yield, and $Y_{C,i}$ refers to the total amount of carbon in the fuel and in the raw gas. The second factor in the numerator accounts for the hydrogen and oxygen that remains in the unconverted char (UC), where $\left[\frac{H}{C}\right]_{UC}$ and $\left[\frac{O}{C}\right]_{UC}$ represent the ratios of the indicated elements. Experimental data for the char yield and its elemental composition have been reported for batch pyrolysis experiments with a similar fuel in a fluidized bed operated at 830°C [29], and these are used as input data to Eq. (2).

Gas yields. In order to facilitate the interpretation of the gas analysis, a conceptual scheme of the gas pathway through the reactor was created. Figure 3 presents the conceptual scheme, whereby the fractions of volatiles and gasification products in contact with the bed are denoted by γ_{vol}^{bed} and $\gamma_{gasif\ prod}^{bed}$, respectively. The initial composition of the volatile pocket released from the fuel particle is assumed to be equal to the pyrolysis gas obtained at the bed temperature. Thereafter, part of the gas may come in contact with the bed, while the remainder escapes without further interaction with the bed particles.

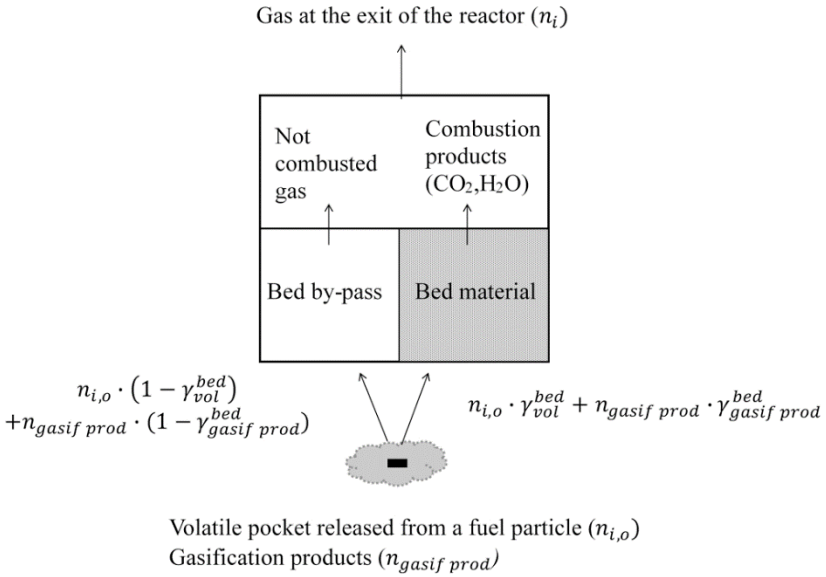

Figure 3. Conceptual schematic of the path taken by combustible gases through the gasifier when an oxygen carrier is used as the bed material.

Ideally, the fraction of gas that contacts the bed is fully oxidized by the MeO, whereas the gas that by-passes the bed may react to some extent with the fluidization steam. Such steam reactions are considered here, since they can take place regardless of the activity of the bed material. In fact, some differences between the pyrolysis gas and raw gas produced *via* steam gasification of wood pellets have been observed in a bed of quartz sand, which is considered to be inert [29]. Those authors reported experimental data for both a pyrolysis gas case ($n_{i,o}$) and a quartz sand case ($n_{i,ref\ sand}$), which are relevant to the present study and are used here for estimation of the gas yields.

According to the proposed conceptual scheme, the theoretical molar yield of the species i at the exit of the gasifier (n_i) can be estimated using a simplified mass balance calculation. Eq. (3) quantifies the gas that by-passes the bed, while Eq. (4) quantifies the combustion products formed by reaction with the oxygen carrier.

$$n_{i,by\ pass} = n_{i,ref\ sand} \cdot \left(1 - \gamma_{vol}^{bed}\right) + \dot{m}_F \cdot Y_{char} \cdot X_{char} \cdot \frac{a_i}{M_{w,i}} \cdot \left(1 - \gamma_{gasif\ prod}^{bed}\right) \quad (3)$$

$$n_{i,bed} = n_{i,o} \cdot \gamma_{vol}^{bed} + \sum_{\substack{j=1 \\ j \neq i}}^{j=N_{species}} \left(n_{j,o} \cdot \gamma_{vol}^{bed} \cdot b_{i,j} + \dot{m}_F \cdot Y_{char} \cdot X_{char} \frac{a_j}{M_{w,j}} \cdot \gamma_{gasif\ prod}^{bed} \cdot b_{i,j} \right)$$

(4)

The corresponding consumed oxygen ($n_{reacted\ MeO}$) is:

$$n_{reacted\ MeO} = \sum_{\substack{j=1 \\ j \neq MeO}}^{j=N_{species}} n_{j,o} \cdot \gamma_{vol}^{bed} \cdot b_{MeO,j} + \dot{m}_F \cdot Y_{char} \cdot X_{char} \frac{\Omega_{S,Char}}{M_{w,O}} \cdot \gamma_{gasif\ prod}^{bed}$$

(5)

The second term in Eqs. (3–5) accounts for the gases derived from char conversion, where a denotes the yield of species $i$or j that is formed *via* char gasification (in units of kg /kg of char). Furthermore, $b_{i,j}$is a stoichiometric coefficient that denotes the amount of species i that is formed by full combustion of the species j (mol i/mol j).

Although char conversion can be quantified, the fraction of gasification products that is combusted ($i.e.\gamma_{gasif\ prod}^{bed}$) remains unknown, so an assumption has to be made. The most conservative assumption has been chosen for Eqs. (3–5), and it refers to fully combusted gasification products ($\gamma_{gasif\ prod}^{bed}$=1). This is the most conservative assumption since it yields the lowest oxygen consumption by the volatiles and thus a lower extent of volatiles-bed contact.

Volatiles conversion. The fraction of volatiles that comes in contact with the bed is estimated by the volatiles conversion factor (X_{vol}), which represents the amount of oxygen consumed by volatile species normalized to the amount of oxygen required for stoichiometric combustion of the volatile matter, and calculated according to:

$$X_{vol} = \frac{\Delta\dot{m}_{O,total} - \dot{m}_F \cdot Y_{char} \cdot X_{char} \cdot \gamma_{gasif\ prod}^{bed} \cdot \Omega_{S,Char}}{\dot{m}_F \cdot \Omega_{SF} - \dot{m}_F \cdot Y_{char} \cdot \Omega_{S,Char}} \qquad (6)$$

The second term in the numerator subtracts the oxygen consumed by the converted char ($\Omega_{S,Char}$). In addition, the two extreme hypotheses for the gasification products ($\gamma_{gasif\ prod}^{bed}$=1 and 0) are evaluated, yielding the maximum and minimum volatile conversions according to Eq. (6).

The net amount of oxygen that is consumed by the fuel ($\Delta\dot{m}_{O,total}$) can be quantified experimentally by the oxygen balance across the gasifier as:

$$\Delta\dot{m}_{O,total} = \left(Y_{O,raw\ gas} - Y_{O,fuel}\right) + \left(Y_{H,fuel} - Y_{H,raw\ gas}\right) \cdot \frac{M_{w,O}}{2 \cdot M_{w,H}} \qquad (7)$$

where the second term accounts for the oxygen that reacts with the hydrogen in the fuel to form water, which is only estimated indirectly from the hydrogen balance.

The choices of notation for volatiles conversion (X_{vol}) and for the theoretical fraction of volatiles in contact with the bed (γ_{vol}^{bed}) were explicitly made in different ways, which means that the measured value may deviate from the ideal case described by Eqs. (3–5). The two parameters are equivalent only if all volatile species react equally fast with the oxygen carrier. However, it has been reported that ilmenite has different reactivities for the various reducing species, reacting faster with H_2 and CO than with CH_4 [21, 24, 30]. Accordingly, high degree of conversion of H_2 and CO have been achieved in pilot-scale CLC reactors, while traces of CH_4 and C_2-C_3 compounds have been measured in the final gas [22, 31]. Therefore, incomplete combustion of the volatile species that contact the bed is anticipated, resulting in an underestimation of the gas-solid contacts by Eq. (6).

In summary, this experimental method provides an estimate of the fraction of volatiles that contacts the bed inventory by quantifying the oxygen consumed by the fuel when the only source of oxygen is the bed material (i.e. an oxygen carrier). The basis of the method is that the oxidation of the fuel occurs by means of heterogeneous gas-solid reaction between

combustible gases released from the fuel and the bed material. A number of errors are introduced by this method, which underestimates the volatile-bed contacts. Uncertainties that need to be considered are the presence of reduced ilmenite in the reactor, the unknown fraction of the gasification products that is combusted, and the variable reactivity of ilmenite for the different gas species.

3. EXPERIMENTAL

The experiments were conducted in a 2-4MW_{th} bubbling bed indirect gasifier at Chalmers University of Technology, which is coupled to a 12-MW_{th} circulating fluidized bed boiler (CFB), as depicted in Figure 4. Since the Chalmers unit has been described in detail elsewhere [29], only a brief description is given here.

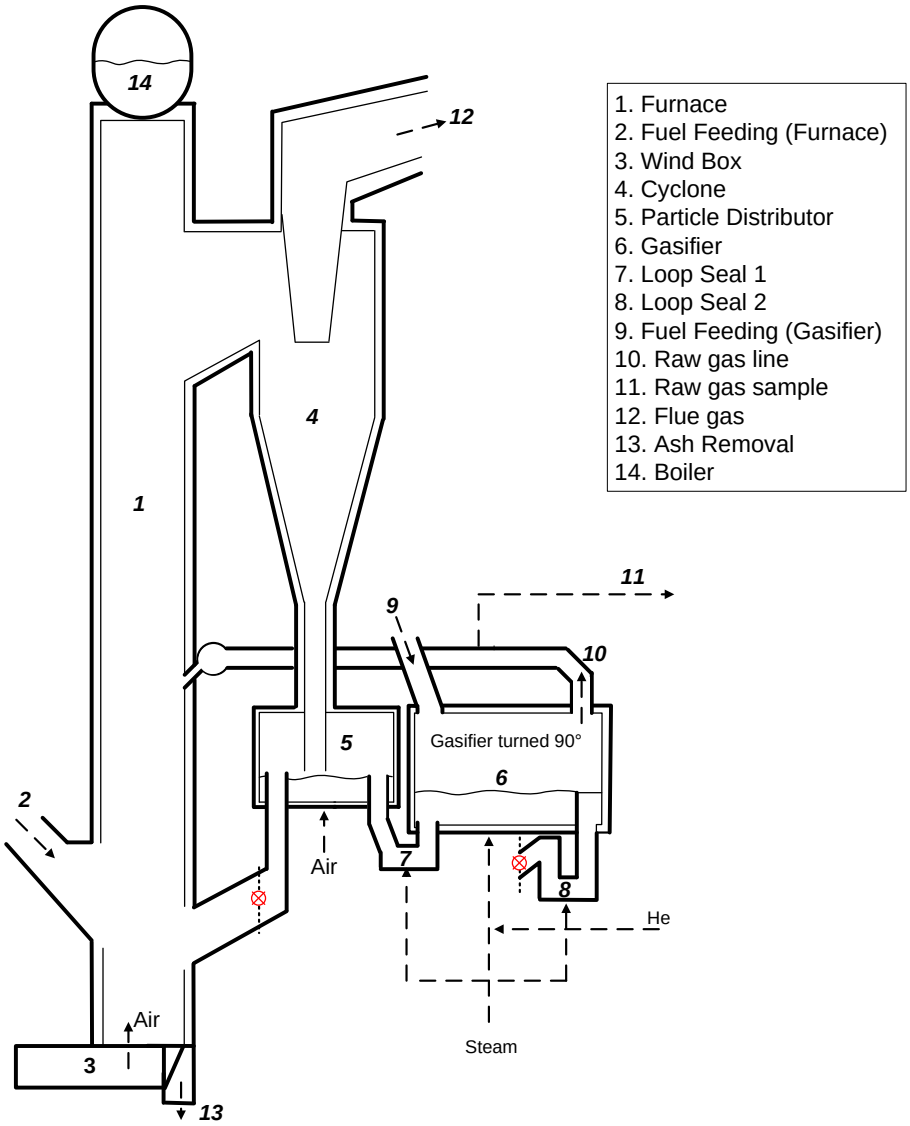

Figure 4. Schematic of the system at Chalmers University of Technology.

The bed material circulates between the furnace (1) and the gasifier (6) *via* a cyclone (4) and an intermediate fluidized bed vessel or particle distributor (5). The particle distributor is usually fluidized with flue gases from the combustor. However, to ensure full oxidation of the ilmenite, this unit was fluidized with air. The oxidized bed material then flows into the gasifier by means of a loop seal (7), and returns to the furnace *via* a second loop seal (8). As shown in Figure 4, both seals and the gasifier were fluidized with steam during the experiments. In addition, a known volume of helium was injected with the fluidization steam to the gasifier, to enable the quantification of total dry gas flow.

In the Chalmers system, the raw gas leaves the gasifier through the raw gas line (10) and returns to the furnace, where it is combusted. A small stream of raw gas (~10 L_n/min) can be continuously sampled from the raw gas line (11), which goes through a ceramic filter at 350°C, to ensure particle removal prior to analysis. Three main sets of gas measurements were conducted on the sampled gas.

- Tar samples were taken according to the solid-phase adsorption (SPA) method, using five 500-mg Supelclean LC-NH2 tubes for each experimental time-point. The samples were eluted and analyzed in a gas chromatograph (BRUKER GC-430) equipped with a midpolar BR-17-ms column and using helium as the carrier gas. The SPA method has proven satisfactory for measuring species heavier than BTX compounds and is less accurate for measuring BTX species [32]. Thus, the results for such heavier species were based on the average value for these five samples. In addition, two SPA samples with both amine and active carbon layers were taken to complement the BTX measurement of each time-point, and the results for the BTX species are based on the average value of these two samples exclusively.
- Char conversion (X_{char}) and total reacted oxygen ($\Delta\dot{m}_{O,total}$) were measured in a High-Temperature Reactor (HTR). In the HTR, the raw gas is heated to 1700°C, so that all the hydrocarbons are decomposed into CO_2, CO, H_2 and H_2O. At the exit of the HTR, the gas is cooled and filtered to remove steam and aerosols, and the dry gas is subsequently measured online. The gas analyzer was a micro-gas chromatograph (micro-GC; Varian Model CP4900) equipped with a molecular sieve (MS5A) and a Poraplot U column, which used argon and helium as the carrier gas, respectively. The total yields of carbon ($Y_{C,raw\ gas}$), hydrogen ($Y_{H,raw\ gas}$), and oxygen ($Y_{O,raw\ gas}$) in the raw gas were derived from the measurements. Detailed descriptions of the reactor

design, measurement technique, and mass balance calculations are provided elsewhere [33].

- In parallel, the permanent gas composition (i.e., He, H_2, CO, CO_2, CH_4, C_2H_2, C_2H_4, C_2H_6, C_3H_6, N_2 and O_2) of a second slipstream of raw gas was analyzed in a micro-GC of the same type as that coupled to the HTR. The columns used were a Poraplot Q and a MS5A, with helium and argon as the carrier gas, respectively. The gas was conditioned prior to analysis by isopropanol quenching and a Peltier cooler was employed for tar and water removal. A detailed description of the gas conditioning system can be found elsewhere [29].

The solids circulation flow ($\dot{m}_{ilm}$) was adjusted by varying the gas velocity at the bottom of the CFB boiler. The solids flow was then measured by temporarily stopping the bed recirculation to the furnace, while monitoring the subsequent decrease in the pressure drop due to the loss of bed inventory, as described previously in [29]. The oxygen availability (λ) was estimated according to Eq. (1), where the bed material was assumed to be fully oxidized at the inlet to the gasifier. The oxygen transport capacity was assumed to be 2.8% by mass, which corresponds to the average of the values reported by others [22-24]. This value provides an order of magnitude of the expected oxygen that can follow with the bed material into the reactor prior experiment.

The bed material was 100% ilmenite, obtained from the processing plant at Pinkenba, Queensland and provided by Sibelco Australia. Despite lower reactivity compared to other oxygen carriers (e.g. synthetic, Cu based materials), ilmenite was chosen as a compromise of reactivity, cost and mechanical strength. The later criteria was significantly relevant given the scale and the duration of the experiment. The density of the material was 4250 kg/m^3 and the diameter of the used particles was in the range of 125–355 μm. Before the experiment was

conducted, the ilmenite inventory was exposed to alternating reducing and oxidizing environment for several days in the same unit. This operation corresponds to more than 40 redox cycles, which is in line with the number of cycles required for activation of ilmenite according to literature [34]. The activation treatment was considered sufficient as stable gas composition was observed the day of the experiment regardless the number of cycles.

The gasifier was fed with wood pellets with the composition shown in Table 1. The assumed data for char yield and its elemental composition are presented in Table 2. The ultimate analysis of the fuel was performed by the Technical Research Institute of Sweden, using the standard methods listed in Table 1. The moisture content was measured by gravimetric analysis of the wet fuel and of the dry fuel after 24 hours at 105°C.

Table 1. Composition of the wood pellets used as the fuel for the gasifier.

Ash (%mass, dry)	**0.4**	**SS-EN 14775**
C (%mass, daf)	**50.30**	**SS-EN 15104**
H (%mass, daf)	6.22	SS-EN 15104
O (%mass, daf)	**43.17**	**By difference**
Moisture (%mass, as received)	8.6	

Table 2. Assumed char data from [29].

Char yield (%mass daf)	**16**
$\left[\frac{H}{C}\right]_{UC}$ **(kgH/kgC)**	0.013
$\left[\frac{O}{C}\right]_{UC}$ **(kgO/kgC)**	0.057

The unconverted fuel from the gasifier is combusted in the combustion side. Additional fuel is added to the later unit (i.e. wood chips). The recirculation of unconverted fuel from the combustor to the gasifier side is negligible compared to the fuel flow to the gasifier. Such recirculation is further minimized by the particle distributor (5 in Figure 4), which acts as an

additional combustion chamber. This ensures that the gas measured in the raw gas line originates from the fuel fed to the gasifier side.

The experimental matrix consisted of four cases (A–D) and two validation tests (A′ and B′), which are summarized in Table 3. In cases A–D, the steam flow was varied at a constant fuel feed to investigate the impact of fluidization on volatiles-bed contacts. The gas velocity was in the range of 0.13–0.28 m/s, which corresponds to 16%–42% of the terminal velocity of the smallest particle size present in the bed inventory (i.e. used particles) in an appreciable quantity. The validation tests (A′ and B′) were conducted to confirm experimentally that the oxygen availability (λ) was sufficiently high not to limit the reaction between volatiles and bed material at the given operating conditions. From the point of view of stoichiometry, if the oxygen carried by the bed material is in excess (λ>1), the conversion of volatiles is expected to be independent of the fuel flow. For this purpose the cases A′ and B′, which were operated with a fuel flow 30% larger than in the cases A-D. As shown in Table 3, this results in an estimated oxygen availability (λ) significantly lower, as well as on a lower bed material flow per unit of fuel. All remaining parameters (i.e. solids flow, and temperature) were kept as similar as possible to the base cases to allow comparison. The steam flows were chosen within the same range tested in cases (A-D).

Table 3. Summary of the experimental matrix.

	Case A	**Case B**	**Case C**	**Case D**	**Case A′**	**Case B′**
Fluidization steam (kg/kg daf fuel)	0.54	0.77	1.00	1.16	0.57	0.81
Fluidization ratio, u_o/u_t*	0.16	0.23	0.30	0.42	0.23	0.33
Fluidization ratio, u_o/u_{mf}**	6	7	9	10	7	10
Bed material flow (kg/kg daf fuel)	86	85	85	85	61	62
Oxygen availability, λ	1.7	1.7	1.7	1.7	1.2	1.2
Average bed temp (°C)	828	824	821	820	827	830

*Calculated for the smallest particle size in the particle size distribution of the used material (i.e. 125μm)

**Calculated for the mean particle size of the used bed material (i.e. 195μm)

For practical reasons, the experiments were conducted on two different days of operation. Cases B, A, C and D were tested in that order on the first day, while Case A′ and Case B′ were tested on the second day. Each experimental point corresponds to approximately 2 hours of operation, which is sufficient time for the system to stabilize and allows for a minimum 30 min of stable gas measurements before the next case was run.

4. RESULTS AND DISCUSSION

The results are based on the average gas measurements obtained during at least 30 min of stable operation, and they are presented in four different sections. The first three sections comprise the investigated uncertainties related to: (1) the catalytic effects owing to the presence of reduced ilmenite, (2) char conversion; and (3) the reactivity of ilmenite towards the different species. In the fourth section, the results for volatiles-bed contacts are summarized, and the errors introduced by the method are assessed.

Catalytic effects by ilmenite. As previously mentioned, the tar yield was measured to gain insights into the relevance of the catalytic and oxidation reactions mediated by the MeO. The results of the tar analysis are shown in Figure 5 as yields of tar species sorted by tar group for Cases A–C, from left to right. The presentation of the tar results by groups was preferred to the total tar to avoid misleading conclusions owing to different conversion rates of the various tar species. A clear trend of decreasing tar yield is observed for all groups as the fluidization velocity increases, with some differences noted for Group 5 compounds.

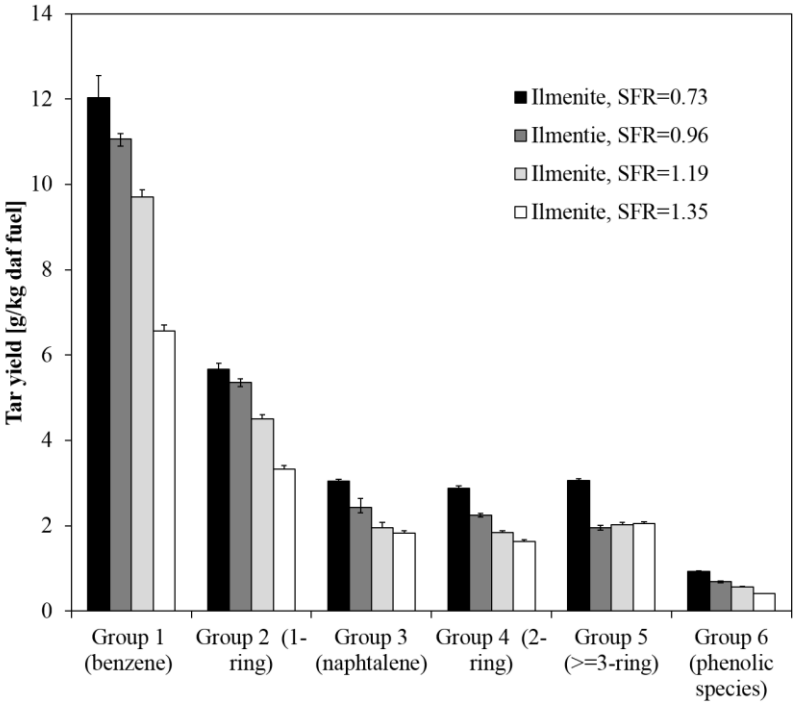

Figure 5. Yields of tar compounds for Cases A–D (increasing gas velocity from left to right).

These results can be explained as the predominance of oxidation reactions caused by the highly oxidized ilmenite, whereas the catalytic effects are minor. This conclusion is in agreement with experimental data reported previously [35], which illustrates a representative case of catalytic behavior by reduced ilmenite (summarized in Fig. 6). The previous experiments were conducted in the same gasifier under similar operational conditions as the present work. The bed material was a blend of 88% quartz sand and 12% ilmenite, which resulted in clear catalytic effects owing to the low oxygen availability (λ~0.12) and the resulting presence of reduced ilmenite in the gasifier. Increases in the yields of all the tar groups were observed when fluidization velocity was increased, which contrasts the trends noted in the present work for highly oxidized ilmenite. Note that due to differences in the tar sampling method only Groups 3–5 are comparable. Furthermore, the rather unchanged levels of Group 5 compounds observed at high fluidization velocities can be interpreted as reflecting a weak catalytic behavior of the bed material. This is in line with the strong tendency of

reduced ilmenite to increase the yield of this tar group (see Fig. 6), which makes it more resilient to the increase in fluidization velocity in the present work.

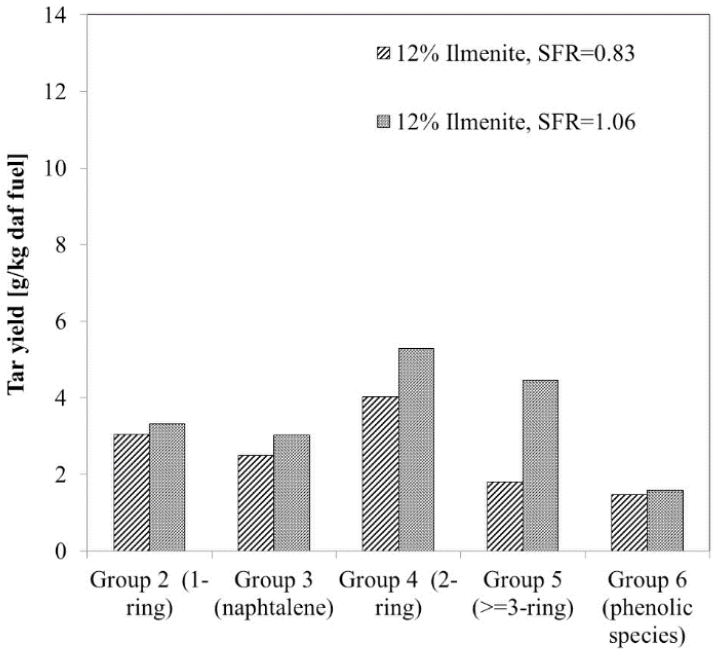

Figure 6. Yields of tar components obtained using a 12% ilmenite-sand bed. Adapted from [35]. Data for benzene were not reported in the original article.

These observations point to combustion reactions being the main pathway for tar decomposition when the bed material is highly oxidized. However, the chemistry of tar is complex, and the roles of the different iron oxides in tar reactions are not clear from the literature. Therefore, further research is needed to understand the interactions between oxygen carriers and tar compounds.

Char conversion. Char conversion was quantified to assess the contribution of gasification products to the measured gas composition. The results for char conversion (X_{char}), derived according to Eq. (2), are shown in Figure 7. Char conversion levels in the range of 0.23–0.27 (weight fraction of the initial char yield) was achieved, which is higher than the reported values (0.0–0.04) from the same gasifier using quartz sand as the bed material [29]. This discrepancy can be attributed to the tendency of volatile species to inhibit char gasification

reactions, which has been investigated by several researchers[36, 37]. In the present experiments, the oxygen carrier acts as a sink for combustible volatiles, creating a gas environment around the char particle that is more favorable to char gasification than in the analogous case with an inert bed material.

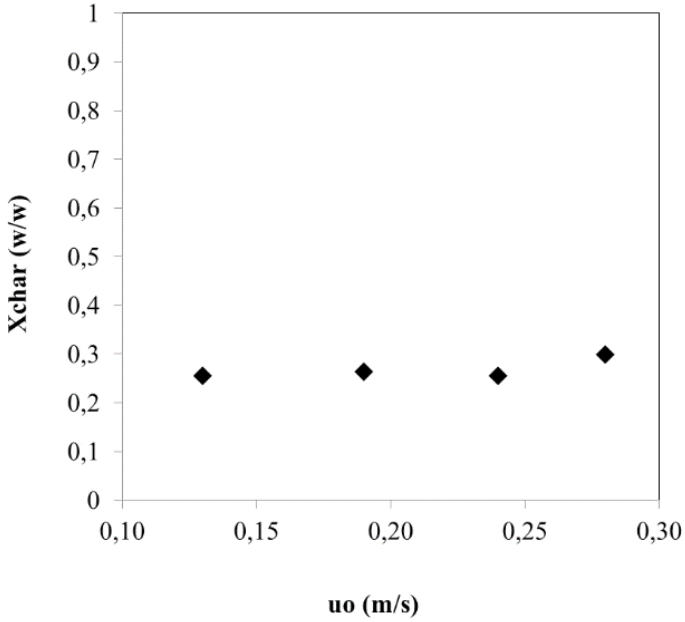

Figure 1. Char conversion level (%mass) in Cases A–D (from left to right).

A remarkable observation is that the steam-to-fuel ratio does not have a significant impact on char conversion, despite the 2-fold increase in fluidization steam from the first case to the last case. Therefore, more research is needed to understand the effect on char conversion of the steam-to-fuel ratio in the presence of oxygen carriers.

Reactivity of ilmenite. The experimental and theoretical gas yields are shown in Figure 8 to 10, assuming complete combustion of the gasification products (i.e., $\gamma_{gasif\ prod}^{bed}$=1). The theoretical yields are calculated using Eqs. (1–3) as a function of the fraction of volatiles that contacts the bed (γ_{vol}^{bed}), whereas the experimental yields are plotted against the measured volatiles conversion (X_{vol}), according to Eq. (5).

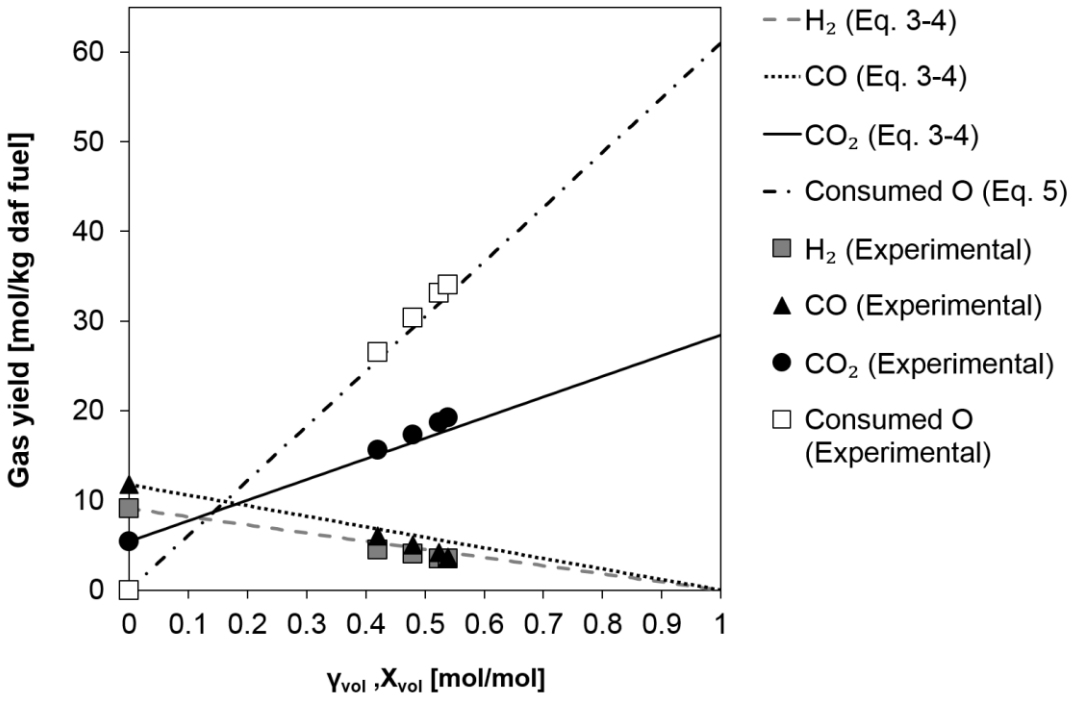

Figure 8. Theoretical (lines, as a function of γvol) and experimental (symbols, as a function of Xvol) molar yields of H2, CO, CO2, and oxygen consumed by volatile species. Full oxidation of gasification products is assumed for the theoretical yields.

Despite the crude simplification of the problem brought about by the proposed conceptual scheme, the experimental data support the expected trends when every contact between the bed material and the volatile species results in complete oxidation of the gases. Note that the yields of CO and H_2 in Figure 9 are generally overestimated, which is in line with the reported higher reactivity of ilmenite towards these two species [36, 37]. This confirms that Eq. (5) gives the minimum measurable fraction of volatiles that comes in contact with the bed, since some of the contacts do not result into combustion products due to the lower reactivity of ilmenite towards some volatile species.

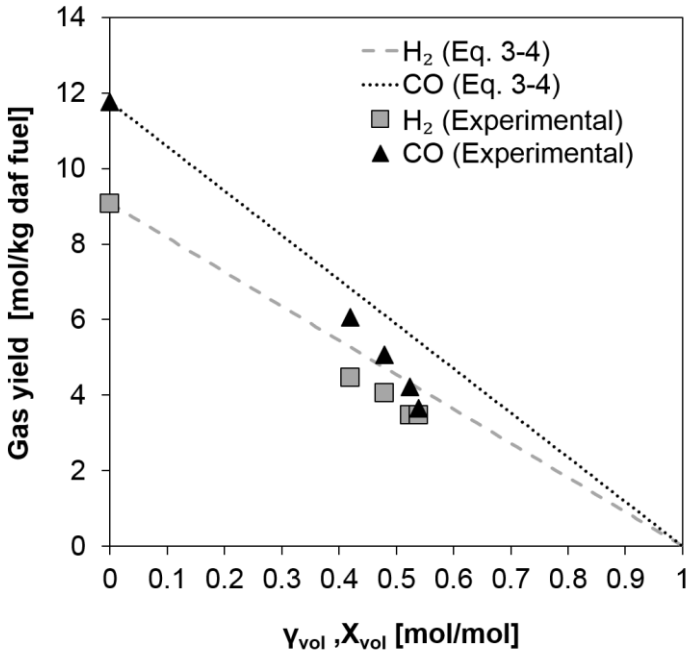

Figure 2. Theoretical (dashed lines as a function of γvol) and experimental (filled symbols as a function of Xvol) molar yields of H_2 and CO as a function of the fraction of volatiles in contact with the bed.

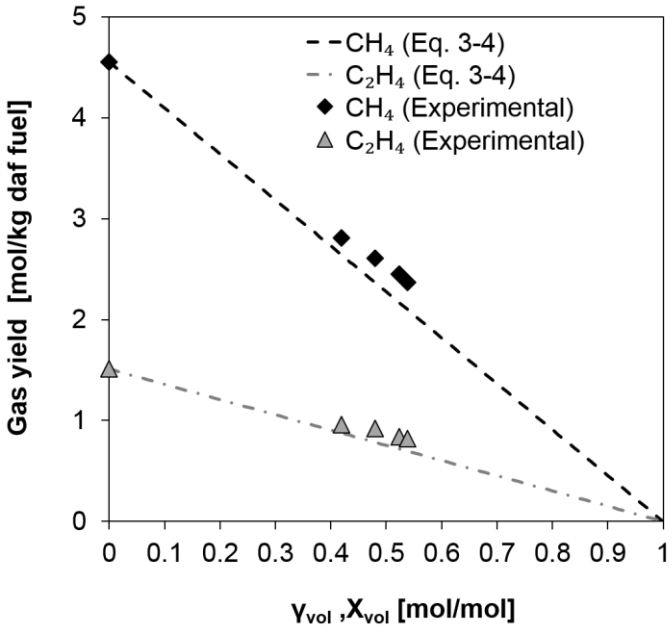

Figure 3. Theoretical (dashed lines as a function of γvol) and measured (filled symbols as a function of Xvol) molar yields of CH4 and C2H4. Full oxidation of gasification products assumed for the theoretical yields.

Volatiles-bed contacts. Figure 11 shows the experimental results for volatiles conversion (X_{vol}) as a function of the fluidization velocity for the different cases, assuming complete combustion of the gasification products (i.e., $\gamma^{bed}_{gasif\ prod}$=1). The cases with low and high fuel flows are shown as filled and open symbols, respectively. The measured conversion level is in the range of 44%–56% for all the cases, and exhibits an upward trend with increasing fluidization velocity. The error bars represent the calculated volatile conversion values if all the gasification products escape the bed (i.e., $\gamma^{bed}_{gasif\ prod}$=0), which results in a relative deviation of 10%–23% depending on the extent of char gasification.

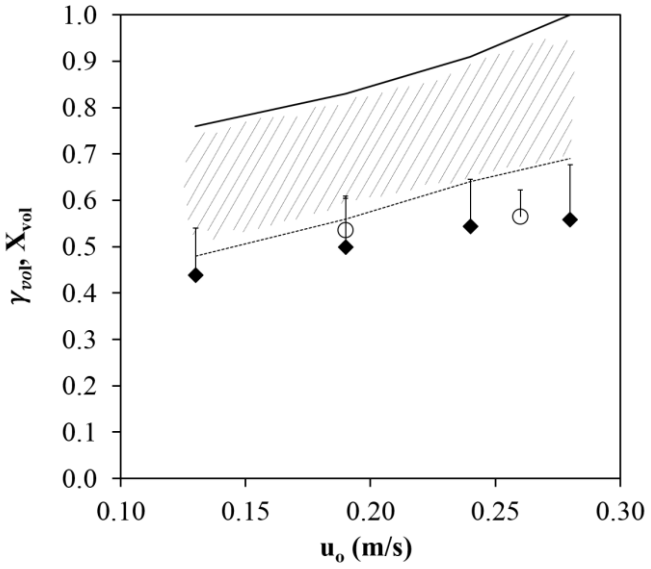

Figure 4. Volatile conversion (Xvol) value calculated according to Eq. (5), assuming $\gamma^{bed}_{gasif\ prod} = 1$; error bars refer to $\gamma^{bed}_{gasif\ prod} = 0$. Filled symbols: Cases A–D; Open symbols: Cases A′ and B′; Striped area: estimated fraction of volatiles in contact with the bed material (γ^{bed}_{vol}) based on CO conversion rates for fully combusted ($\gamma^{bed}_{gasif\ prod} = 1$) and fully uncombusted ($\gamma^{bed}_{gasif\ prod} = 0$) gasification products.

The validation tests (Case A′ and Case B′) confirm that the oxygen availability was sufficient throughout all the experiments, which means that incomplete combustion was not caused by a shortage of oxygen carrier in the gasifier. The slightly higher values noted for Cases A′ and B′, as compared with the low-fuel cases, can be attributed to the somewhat higher temperature

of the bed material, or to changes in the fluid dynamics of the bed that resulted from the higher concentration of devolatilizing fuel particles in the reactor.

The uncertainty related to the variable reactivity of ilmenite for the different combustible gases is indicated by the striped area in Figure 11. The uncertainty was evaluated by testing the two extreme hypotheses for char gasification products in Eq. (1), which result in the upper and lower limit of the striped area. The experimental yield of CO was used as input data, since it is the species that exhibits the highest conversion rate. The upper boundary (i.e., $\gamma_{gasif\ prod}^{bed}$=0) is, however, unrealistic since part of the gasification products are most likely combusted by the bed material. In fact, >97% conversion of wood char gasification products has been recently reported for a 100-kW CLC unit operating with ilmenite [38]. In the present work, the conversion level is expected to be even higher, provided that the fuel particles are significantly larger than the ones used in the mentioned work (i.e., 200–1000 μm). Note that the gas measurements also agrees fairly well with the assumption of fully combusted gasification products as shown on Figs 8 to 10.Therefore, the most plausible solution is instead close to the lower limit of the striped area in Figure 11. This results in a gas-solid contact level that is 7%–12% higher than the corresponding measured volatiles conversion (X_{vol}).

The present measurements show that significant mixing between the volatiles released from a fuel particle and the bed material can be expected in bubbling bed reactor despite the fuel was fed on the top of the bed. The method does not provide information about the nature of the movement experienced by the fuel particles, nor about the region where the contact takes place. According to the segregation/mixing literature it is expected that the devolatilizing fuel locate in the upper region of the bubbling bed[14]. Consequently, the relatively high conversion of volatiles is most likely the result of the intense mixing in the splash region induced by the bubbles bursting at the surface of the fluidized bed. The increasing fluidization velocity

contributes to a more agitated splash zone as it is illustrated in Figure 1, which is in line with the increasing extent of contact between volatiles and the bed material shown in the results.

The values obtained for volatiles-bed contact must be interpreted with care, since the volatile conversion level that can be achieved with a different bed material depends also on the inherent reactivity of the bed material itself. For instance, higher bed temperature and smaller particles size of the bed material would presumably increase the reactivity of the ilmenite and, thereby, the effective volatile-bed contact. This indicates that the values presented here are the minimum volatile-bed contact that could be measured at the operating conditions investigated.

5. CONCLUSIONS

Volatiles-bed contacts were investigated in a 2-4MW_{th} bubbling bed gasifier with an over-bed fuel-feeding system, and using full size wood pellets as fuel (300–400 kg/h). An experimental method to estimate the fraction of volatiles that contacts the bed material was developed, and the main uncertainties were investigated. The impact of fluidization velocity was explored within the bubbling regime, and the range of gas velocities tested was 6–10-times the value of u_{mf}. The following conclusions are drawn from the results:

- The method provides the minimum value for the fraction of volatiles that comes in contact with the bed material.
- The major uncertainties relate to the unknown fraction of char gasification products that contacts the bed material, as well as the variable reactivity of the bed material for the various species;
- At the lowest fluidization velocity tested (i.e., 6-times the u_{mf}), at least 48% of the volatiles are estimated to come in contact with the solids;

- The mixing of volatiles is enhanced by an increase in fluidization velocity, with at least 69% of the volatiles coming in contact with the bed at the highest fluidization velocity tested (i.e., 10-times the u_{mf}).

The experimental results indicate that a significant fraction of the volatiles released from a large fuel particle is in contact with the bed material in a bubbling bed reactor. This finding reveals a great potential for in-bed tar removal methods in bubbling bed gasifiers, even with an over-bed fuel-feeding system.

AUTHOR INFORMATION

Corresponding Author

* Tel:+46(0) 31 772 14 55, E-mail: berdugo@chalmers.se

ACKNOWLEDGMENTS

This work has been financially supported by the Swedish Gasification Center (SFC) and E.On. We thank Jelena Marinkovic and Mikael Israelsson for their help during the measurements, as well as Fredrik Lind for his help running the unit and discussions. The authors also acknowledge the technical assistance by the research engineers Jessica Bohwalli, Johannes Öhlin and Rustan Marberg.

REFERENCES

1. D. Kunii and O. Levenspiel, *Fluidization Engineering (Second Edition)*, Butterworth-Heinemann, Boston, **1991**.
2. J. Koornneef, M. Junginger and A. Faaij, *Progress in Energy and Combustion Science*, **2007**, 33, 19-55.
3. P. Kaushal and R. Tyagi, *The Canadian Journal of Chemical Engineering*, **2012**, 90, 1043-1058.
4. J. Adanez, A. Abad, F. Garcia-Labiano, P. Gayan and L. F. de Diego, *Progress in Energy and Combustion Science*, **2012**, 38, 215-282.
5. D. Sutton, B. Kelleher and J. R. H. Ross, *Fuel Processing Technology*, **2001**, 73, 155-173.
6. L. Devi, K. J. Ptasinski and F. J. J. G. Janssen, *Biomass and Bioenergy*, **2003**, 24, 125-140.
7. C. Pfeifer, J. C. Schmid, T. Pröll and H. Hofbauer, in *Proc. 19th European Biomass Conference and Exhibition*, Berlin, Germany, **2011**.
8. J. C. Schmid, T. Pröll, C. Pfeifer and H. Hofbauer, in *Proc. 9th European Conference on Industrial Furnaces and Boilers (INFUB)*, Estoril, Portugal, **2011**.

9. V. Wilk, J. C. Schmid and H. Hofbauer, *Biomass and Bioenergy*, **2013**, 54.
10. J. R. Grace, *The Canadian Journal of Chemical Engineering*, **1986**, 64, 353-363.
11. P. N. Rowe and A. W. Nienow, *Powder Technology*, **1976**, 15, 141-147.
12. G. Bruni, R. Solimene, A. Marzocchella, P. Salatino, J. G. Yates, P. Lettieri and M. Fiorentino, *Powder Technology*, **2002**, 128, 11-21.
13. R. Solimene, A. Marzocchella and P. Salatino, *Powder Technology*, **2003**, 133, 79-90.
14. M. Fiorentino, A. Marzocchella and P. Salatino, *Chemical Engineering Science*, **1997**, 52, 1909-1922.
15. A. Gómez-Barea and B. Leckner, *Progress in Energy and Combustion Science*, **2010**, 36, 444-509.
16. F. Scala and P. Salatino, *Chemical Engineering Science*, **2002**, 57, 1175-1196.
17. R. Irusta, G. Antolin, E. Velasco and R. De Miguel, *Fluidization VIIII, Engineering Foundation, New York*, **1995**, 855-862.
18. V. A. Borodulya, V. I. Dikalenko, G. I. Palchonok and L. K. Stanchits, *Fluidized bed combustion of solid organic wastes and low-grade coals: Research and modeling*, **1995**.
19. F. Scala and R. Chirone, *Experimental Thermal and Fluid Science*, **2004**, 28, 691-699.
20. A. Lyngfelt, in *Fluidized Bed Technologies for Near-Zero Emission Combustion and Gasification*, Woodhead Publishing, **2013**, pp. 895-930.
21. A. Cuadrat, A. Abad, J. Adánez, L. F. de Diego, F. García-Labiano and P. Gayán, *Fuel Processing Technology*, **2012**, 94, 101-112.
22. T. Mendiara, A. Abad, L. F. de Diego, F. García-Labiano, P. Gayán and J. Adánez, *International Journal of Greenhouse Gas Control*, **2013**, 19, 322-330.
23. J. Adánez, A. Cuadrat, A. Abad, P. Gayán, L. F. de Diego and F. García-Labiano, *Energy & Fuels*, **2010**, 24, 1402-1413.
24. A. Abad, J. Adánez, A. Cuadrat, F. García-Labiano, P. Gayán and L. F. de Diego, *Chemical Engineering Science*, **2011**, 66, 689-702.
25. M. Virginie, J. Adánez, C. Courson, L. F. de Diego, F. García-Labiano, D. Niznansky, A. Kiennemann, P. Gayán and A. Abad, *Applied Catalysis B: Environmental*, **2012**, 121-122, 214-222.
26. K. Polychronopoulou, A. Bakandritsos, V. Tzitzios, J. L. G. Fierro and A. M. Efstathiou, *Journal of Catalysis*, **2006**, 241, 132-148.
27. L. Di Felice, C. Courson, P. U. Foscolo and A. Kiennemann, *International Journal of Hydrogen Energy*, **2011**, 36, 5296-5310.
28. M. Azhar Uddin, H. Tsuda, H. Tsuda, S. Wu and E. Sasaoka, *Fuel*, **2008**, 87, 451-459.
29. A. Larsson, M. Seemann, D. Neves and H. Thunman, *Energy & Fuels*, **2013**, 27.
30. G. L. Schwebel, S. Sundqvist, W. Krumm and H. Leion, *Journal of Environmental Chemical Engineering*, **2014**, 2.
31. H. Gu, L. Shen, J. Xiao, S. Zhang and T. Song, *Energy & Fuels*, **2010**, 25, 446-455.
32. M. Israelsson, M. Seemann and H. Thunman, *Energy & Fuels*, **2013**, 27, 7569-7578.
33. M. Israelsson, A. Larsson and H. Thunman, *Energy & Fuels*, **2014**, 28, 5892-5901.
34. G. L. Schwebel, H. Leion and W. Krumm, *Chemical Engineering Research and Design*, **2012**, 90, 1351-1360.
35. A. Larsson, M. Israelsson, F. Lind, M. Seemann and H. Thunman, *Energy & Fuels*, **2014**, 28, 2632-2644.
36. M. Keller, H. Leion, T. Mattisson and A. Lyngfelt, *Combustion and Flame*, **2011**, 158, 393-400.
37. B. Bayarsaikhan, N. Sonoyama, S. Hosokai, T. Shimada, J.-i. Hayashi, C.-Z. Li and T. Chiba, *Fuel*, **2006**, 85, 340-349.
38. C. Linderholm, M. Schmitz, P. Knutsson, M. Källén and A. Lyngfelt, *Energy & Fuels*, **2014**, 28, 5942-5952.